Identification of a Model Cardiac Glycoside Receptor: Comparisons with Na^+,K^+-ATPase†

Rama Kasturi,‡ Jie Yuan,‡ Larry R. McLean,§ Michael N. Margolies,|| and William J. Ball, Jr.*,‡

Department of Pharmacology and Cell Biophysics, University of Cincinnati, Cincinnati, Ohio 45267, Hoechst Marion Roussel Inc., Cincinnati, Ohio 45215, and Department of Surgery, Massachusetts General Hospital, Boston, Massachusetts 02114

Received December 11, 1997; Revised Manuscript Received March 11, 1998

ABSTRACT: The availability of high-affinity anti-digoxin monoclonal antibodies (mAbs) offers the potential for their use as models for the characterization of the relationship between receptor structure and cardiac glycoside binding. We have characterized the binding of anthroylouabain (AO), a fluorescent derivative of the cardiac glycoside ouabain, to mAbs 26-10, 45-20, and 40-50 [Mudgett-Hunter, M., et al. (1995) *Mol. Immunol. 22*, 477] and lamb kidney Na^+,K^+-ATPase by monitoring the resultant AO fluorescence emission spectra, anisotropy, lifetime values, and Förster resonance energy transfer (FRET) from protein tryptophan(s) (Trp) to AO. These data suggest that the structural environment in the vicinity of the AO-binding site of Na^+,K^+-ATPase is similar to that of mAb 26-10 but not mAbs 45-20 and 40-50. A model of AO complexed to the antigen binding fragment (Fab) of mAb 26-10 which was generated using known X-ray crystal structural data [Jeffrey, P. D., et al. (1993) *Proc. Natl. Acad. Sci. U.S.A. 90*, 10310] shows a heavy chain Trp residue (Trp-H100) that is close (∼3 Å) to the anthroyl moiety. This is consistent with the energy transfer seen upon AO binding to mAb 26-10 and suggests that Trp-H100, which is part of the antibody's cardiac glycoside binding site, is a major determinant of the fluorescence properties of bound AO. In contrast, the generated model of AO complexed to Fab 40-50 [Jeffrey, P. D., et al. (1995) *J. Mol. Biol. 248*, 344] shows a heavy chain Tyr residue (Tyr-H100) which is part of the cardiac glycoside binding site, located ∼10 Å from the anthroyl moiety. The closest Trp residues (H52 and L35) are located ∼17 Å from the anthroyl moiety, and no FRET is observed despite the fact that these Trp residues are close enough for significant FRET to occur. The energy transfer seen upon AO binding to Na^+,K^+-ATPase suggests the presence of one completely quenched or two highly quenched enzyme Trp residues ∼10 and ∼17 Å, respectively, from the anthroyl moiety. These data suggest that the Na^+,K^+-ATPase Trp residue-(s) involved in fluorescence energy transfer to AO is likely to be part of the cardiac glycoside binding site.

Na^+,K^+-ATPase[1] is a P-type ATPase (*1*, *2*) characterized by the formation of a phosphoenzyme intermediate during the catalytic cycle. This transmembrane protein pump, found in the plasma membrane of higher eukaryotic cells, is responsible for transporting Na^+ and K^+ ions across cell membranes against their respective cellular gradients using the energy derived from ATP hydrolysis (see ref *3* for review). The minimal functional unit of the enzyme is a heterodimer composed of a catalytic (α) subunit and a glycoprotein (*β*) subunit with approximate molecular masses of 113 and 55 kDa, respectively. The α subunit contains the phosphorylation site and the binding sites for Na^+, K^+, Mg^{2+}, ATP, and cardiac glycosides. Although it is essential for an active enzyme (*4*−*6*), the physiological function of *β* remains unclear.

Unlike other P-type ATPases, Na^+,K^+-ATPase is specifically inhibited by cardiac glycosides, a class of steroids with an unsaturated lactone at the 17*β* position and a sugar moiety at the 3*β* position. Cardiac glycosides are frequently used in the treatment of congestive heart failure and some arrhythmias as their inhibition of Na^+,K^+-ATPase activity results in an increase in the force of myocardial contractility or positive inotropy (see ref *7* for review).

Despite considerable study, neither the three-dimensional structure of Na^+,K^+-ATPase nor the site of cardiac glycoside binding has been determined. Although binding of cardiac glycosides to Na^+,K^+-ATPase occurs extracellularly (*8*) in the presence of Mg^{2+} alone, these drugs bind with the highest affinity upon formation of a phosphoenzyme intermediate in the presence of either Na^+ and Mg^{2+}-ATP or Mg^{2+} and

† This work was supported by NIH Training Grant 5 T32 HLO7382 (R.K.), NIH Grant RO1 HL-50613 (J.Y. and Dr. Earl T. Wallick), an American Heart Association Ohio affiliate grant-in-aid (W.J.B.), and NIH Grant RO1 HL-47415 (M.N.M.).

* To whom correspondence should be addressed: Department of Pharmacology and Cell Biophysics, University of Cincinnati College of Medicine, 231 Bethesda Ave., Cincinnati, OH 45267-0524. Telephone: (513) 558-2388. Fax: (513) 558-1169. E-mail: william.ball@uc.edu.

‡ University of Cincinnati.

§ Hoechst Marion Roussel Inc.

|| Massachusetts General Hospital.

[1] Abbreviations: Na^+,K^+-ATPase, magnesium-dependent and sodium- and potassium-activated adenosine triphosphatase (EC 3.6.1.37); AO, anthroylouabain; Fab, antigen-binding fragment; mAb, monoclonal antibody; L and H, antibody light and heavy chains, respectively; PBS, phosphate-buffered saline; BSA, bovine serum albumin; EGTA, ethylene glycol bis(*β*-aminoethyl ether)-*N*,*N*,*N*′,*N*′-tetraacetic acid; IC_{50}, inhibitory concentration of glycoside required to produce a 50% decrease in [^{3}H]digoxin binding to antibody; FRET, Förster resonance energy transfer; *r*, fluorescence anisotropy; τ_{av}, average fluorescence lifetime; FITC, fluorescein 5′-isothiocyanate; ErITC, erythrosin 5′-isothiocyanate; 5′-IAF, 5′-iodoacetamidofluorescein.

S0006-2960(97)03037-7 CCC: $15.00
Published on Web 04/18/1998

inorganic phosphate (P_i) (*9*). Studies using photoaffinity analogues of glycosides have established the α subunit as the primary site of binding, although low levels of photolabeling of the *β* subunit have also been observed (for review, see refs *10* and *11*). Additionally, chemical modification studies of Na^+,K^+-ATPase using protein reactive derivatives of digoxigenin (*12*) have implicated the NH_2-terminal half of the enzyme's α subunit in cardiac glycoside binding. Numerous site-directed mutagenesis studies using the ouabain-sensitive sheep or *Xenopus laevis* Na^+,K^+-ATPase α1 isoform (*13*−*22*) have revealed that multiple amino acid residues in the putative extracellular H1−H2, H3−H4, and H7−H8 loops and H1 and H5 transmembrane regions of the α subunit are involved in determining the enzyme's ouabain sensitivity. However, it is still unclear whether the effects of these mutations on enzyme sensitivity to inhibition by ouabain result from these residues being part of the binding site or their indirect regulation of cardiac glycoside binding via induced conformational changes in the α subunit (*3*). In addition, studies of chimeras of the α subunits of Na^+,K^+-ATPase and H^+,K^+-ATPase (*23*) or Ca^{2+}-ATPase (*24*) have established that large domains at both the NH_2- and COOH-terminal regions of the Na^+,K^+-ATPase are necessary for achieving high-affinity ouabain binding.

Although the Na^+,K^+-ATPase is the only known physiological receptor for cardiac glycosides, high-affinity polyclonal anti-digoxin antibodies have been generated and used clinically since 1976 to monitor serum digoxin levels and to reverse digitalis toxicity in patients (*25*). Subsequently, a number of murine monoclonal antibodies (mAbs) that bind digoxin and other cardiac glycosides with high affinities and differing specificities have been isolated and studied in detail to determine the correlation between mAb structure and glycoside binding specificity (*26*). The recent determination of the crystal structures of the antigen binding fragments (Fabs) of mAbs 26-10 and 40-50 with and without bound digoxin/ouabain (*28*, *29*) and the availability of bacteriophage-displayed 26-10 Fab and libraries of random mutant variants (*30*) allow the use of these mAbs as novel model receptors for further characterizations of the relationship between protein structure and cardiac glycoside binding. The idiotype network theory of Jerne (*31*), which proposes that an antibody should duplicate a receptor-like binding site to effect a high-affinity interaction with a receptor ligand which serves as the antibody's antigen, lends further support to the concept of utilizing these anti-digoxin mAbs as potential model digitalis receptors.

The objective of this study was to determine whether, in fact, anti-digoxin mAbs can serve as models of the physiological digitalis receptor by using a fluorescent ouabain derivative, anthroylouabain (AO), which is a specific, high-affinity probe of the cardiac glycoside site of Na^+,K^+-ATPase (*32*, *33*), to investigate the environment of the cardiac glycoside binding domains in mAbs and enzyme. We have compared the steady-state and dynamic fluorescence properties of AO bound to Na^+,K^+-ATPase and to mAbs 26-10, 45-20, and 40-50. Of the three mAbs studied, only the binding of mAb 26-10 to AO was similar to that of Na^+,K^+-ATPase. As the relationship between antibody structure and cardiac glycoside binding to this mAb is known, this information may be used to facilitate construction of a model(s) of cardiac glycoside (AO) binding to Na^+,K^+-ATPase.

MATERIALS AND METHODS

Purification of Na^+,K^+-ATPase. Na^+,K^+-ATPase was purified from the outer medulla of frozen lamb kidney according to the method of Lane et al. (*34*). The initial activity of the enzyme was ∼900 to 1100 *μ*mol of ATP hydrolyzed (mg of protein)$^{-1}$ h^{-1}. The enzyme concentration was determined by the Lowry procedure (*35*), using BSA as the protein standard.

Monoclonal Antibody Production. Monoclonal anti-digoxin antibody-producing cell lines 26-10 (γ_{2a}, κ), 45-20 (γ_{2a}, λ_1), and 40-50 (γ_{2b}, κ) were obtained through fusion of immune A/J splenocytes with the nonsecreting cell line Sp/2/0 Ag 14 (*26*). Anti-digoxin monoclonal antibodies were purified from ascites by affinity chromatography on ouabain−amine−Sepharose and their purities assessed by SDS−polyacrylamide gel electrophoresis (*26*). The purified mAbs were dialyzed exhaustively against PBS containing 0.02% sodium azide to remove bound ouabain, and their concentrations were determined using an $E^{0.1\%}_{280}$ of 1.4.

Affinity of mAbs for Digoxin, Ouabain, and Anthroylouabain. A competition radioligand binding assay utilizing double antibody precipitation was used to measure mAb affinity for digoxin, ouabain, and anthroylouabain. Purified mAb (0.006 *μ*g/assay) was incubated at room temperature for 1 h with 5 nM [^{3}H]digoxin (specific activity = 15 Ci/mmol, Dupont New England Nuclear, Boston, MA) and varying concentrations of competing ligand (cold digoxin, ouabain, or anthroylouabain) in 0.5 mL of phosphate-buffered saline (pH 7.4) containing 0.05% BSA. A 5-fold molar excess of an affinity-purified goat anti-mouse IgG Fc-specific antibody (ICN Biomedicals) was then added to each assay tube, and the binding reactions were allowed to go to completion by incubating the tubes overnight at 4 °C. The following morning, a 10-fold molar excess (over the goat anti-mouse IgG) of an affinity-purified rabbit anti-goat IgG antibody was added and the samples were incubated at room temperature for 2 h. Ice-cold phosphate-buffered saline (8 mL) was then added to each assay tube, and the suspension was filtered under vacuum through glass fiber filters (24 mm, no. 32, Schleicher & Schuell, Inc., Keene, NH). The filters were subsequently washed twice with 8 mL of buffer and incubated overnight at room temperature in 8 mL of scintillation fluid (Fisher Scientific) prior to counting in a liquid scintillation counter. To determine the amount of nonspecific binding, 0.006 *μ*g of an anti-Na^+,K^+-ATPase α subunit mouse mAb, M7-PB-E9 (*36*), was incubated with 5 nM [^{3}H]digoxin in the same buffer. The IC_{50} values of the three glycosides for each mAb were obtained by fitting the radioligand binding data (two data sets obtained in duplicate) with a nonlinear competition binding curve using Inplot (GraphPad, SanDiego, CA). These IC_{50} values were then converted to inhibitory dissociation constants (K_i's), using the equation of Cheng and Prusoff (*37*), $K_i = IC_{50}/(1 + [L]/K_d)$, where [L] is the concentration of the [^{3}H]digoxin used and K_d is the dissociation constant of mAb for digoxin. The K_d values of mAbs for digoxin were obtained using the experimental protocol outlined above, except that mAb (0.006 *μ*g/assay) was incubated with varying concentrations of [^{3}H]digoxin in the absence of any competing ligand. The radioligand binding data were analyzed using PRISM (GraphPad), a nonlinear regression

curve fitting program, to obtain the K_d values of mAbs for digoxin.

Fluorescence Measurements. An SLM/Aminco SPF-500C spectrofluorometer (Urbana, IL) was used to obtain the fluorescence spectra of free and protein-bound AO. Prior to measurements of fluorescence, AO (0.3 μM) was incubated with a 2-fold molar excess of Na^+,K^+-ATPase and mAbs for 10−15 min at 25 °C, unless specified otherwise, in 50 mM Tris-HCl buffer (pH 7.4) and 1 mM EGTA, with and without 5 mM $MgCl_2$ and P_i, respectively. Excess unlabeled ouabain (60 μM) was added to the AO−protein samples to determine the extent of nonspecific binding of AO, if any, and to correct for it. The excitation (λ_{ex}) and emission (λ_{em}) wavelengths used for AO were 364 and 485 nm, respectively. Band-pass widths for excitation and emission were set at 4 and 10 nm, respectively.

Polarization data were obtained using an ISS (Industria Strumentazioni Scientifiche, Champaign, IL) Greg K2 spectrofluorometer. AO (0.3 μM) was incubated with increasing concentrations of protein at 37 °C for 10−15 min prior to initiating fluorescence intensity measurements. The fluorescence of AO was excited at $\lambda_{ex} = 360$ nm using a xenon arc lamp with an Ealing 35-3037 interference filter on the excitation side. Fluorescence emission was observed through a Schott glass 417 kV cutoff filter. Polarization data were obtained by exciting the samples with vertically polarized light and observing the emission intensities through a polarized filter oriented first in the vertical (I_v) and then the horizontal (I_h) position. The total fluorescence intensity was calculated with $I = I_v + 2I_h$ and the anisotropy (r) value with $r = [(I_v/I_h) - G)]/[(I_v/I_h) + 2G]$, where G is the instrumentation factor that corrects the r value for the unequal detection by the fluorometer of vertically and horizontally polarized light (*38*).

Förster Resonance Energy Transfer Measurements (FRET). Steady-state determinations of acceptor (AO)-dependent quenching of donor (protein Trp) fluorescence and concurrent enhancement of AO fluorescence occurring with the Trp−AO pair were made using an SLM/Aminco SPF-500C spectrofluorometer with a λ_{ex} of 295 nm and band-pass widths for excitation and emission set at 4 and 10 nm, respectively. AO (0.3 μM) was incubated with excess protein (0.6 μM) for 10−15 min at 25 °C, in 50 mM Tris-HCl (pH 7.4) and 1 mM EGTA, with or without 5 mM $MgCl_2$ and P_i. The Förster critical distance, R_0, which is the distance between the donor (D) and acceptor (A) pair at which the donor excitation energy is transferred with 50% efficiency, was calculated using the equation R_0 (centimeters) $= (9.79 \times 10^{-5})(J\eta^{-4}\kappa^2\phi_D)^{1/6}$ (*38*, *39*), where J is the overlap integral between the donor emission and the acceptor absorption spectra, η is the refractive index of the solution, κ^2 is the orientation factor of the emission (donor) and absorption (acceptor) dipoles, and ϕ_D is the quantum yield of the donor in the absence of acceptor. The fluorescence quantum yield of the donor (Trp) in the absence of acceptor (AO) was estimated using *N*-acetyl-L-tryptophanamide as the standard ($\phi_{std} = 0.13$). The values of η, ϕ_D , J, and κ^2 used to determine R_0 were as follows: $\eta = 1.33$ (refractive index of a dilute aqueous solution), $\phi_D = 0.1$, $J = 5.2 \times 10^{-15}$ cm^3/M [acceptor extinction coefficient (ϵ) = 7800 M^{-1} cm^{-1}], and $\kappa^2 = {}^2/_3$ (*38*) (assuming random orientations of the donor and acceptor dipoles before energy transfer). The percent efficiency (E) of energy transfer was calculated with $E = 1 - (F/F_0)$, where F and F_0 are the donor fluorescence intensities in the presence and absence of acceptor, respectively. Estimates of the distance (R) between the donor and acceptor pair were calculated from the efficiency of energy transfer using the equation $R = R_0[(1 - E)/E]^{1/6}$.

Fluorescence Lifetimes. AO fluorescence lifetimes were measured by the phase-modulation technique (*38*) using an ISS (Industria Strumentazioni Scientifiche) Greg K2 spectrofluorometer. AO was excited by an argon ion laser (Coherent Inova 300) (333.6−363.8 nm) with a Pockel cell as a light modulator over the 2−200 MHz frequency range. The fluorescence emission of 0.8 μM AO alone and AO complexed with mAbs 26-10 and 45-20 (1.0−1.2 μM) or Na^+,K^+-ATPase (1.6 μM) was observed through a Schott glass 418 kV cutoff filter. Magic angle polarizer conditions were used, and the temperature of the samples was held at 25 °C by a circulating water bath. An aqueous suspension of LUDOX (Aldrich Chemical Co.) was used as the reference sample. A nonlinear least-squares fitting program (ISS, Inc.) was used to analyze the phase and modulation data in terms of single-, double-, and triple-exponential decays. Phase (ϕ) and modulation (m) data were fit by minimizing the χ^2 (goodness-of-fit) parameter (*40*). For all analyses, the uncertainties in the phase and modulation values obtained were taken to be 0.2 and 0.004, respectively.

Modeling of AO Binding to Antigen-Binding Fragments (Fabs) of mAbs 26-10 and 40-50. Models of AO binding to mAbs 26-10 and 40-50 were generated using the known X-ray crystal structures of the Fab 26-10−digoxin (*28*) and Fab 40-50−ouabain (*29*) complexes. Digoxin and ouabain were first converted to AO by modification of the appropriate atoms while keeping the structure of the rest of the drug−Fab complex intact. Structure refinement (energy minimization) and conformational searches (dynamics simulations) of the models were then performed by Discover (Biosym/MSI, San Diego, CA) using the consistent valence force field (CVFF), to generate the most probable, thermodynamically favorable structures. The following parameters were employed in the calculations: overlap distance = 0.01 Å, upper limit of the cutoff distance (cutoff) = 20.0 Å, lower limit of the cutoff distance (cutdis) = 19.0 Å, switching distance = 1.5 Å, distance-dependent dielectric = 1.0r, no cross term, and no Morse. For all dynamics simulations, the AO−Fab models were heated to 300 K and pre-equilibrated for 500 iterations before data collection (10 000 iterations, snapshots taken at 100 iteration intervals). The models were then cooled slowly to 0 K with an exponential decay constant of 0.5 ps (5000 iterations) and a step size of 1 fs. Graphical displays were generated by Insight II (Biosym/MSI).

Materials. Digoxin and anthroylouabain were purchased from Sigma Chemical Co. Ouabain was purchased from Boehringer Mannheim. [^{3}H]Digoxin was purchased from Dupont New England Nuclear. All other materials used were reagent grade.

RESULTS

Determination of mAb Affinities (K_i) for AO. The affinities of mAbs 26-10, 45-20, and 40-50 were determined as a prerequisite for using the fluorescent ouabain derivative, anthroylouabain (AO), as a probe of the physical properties

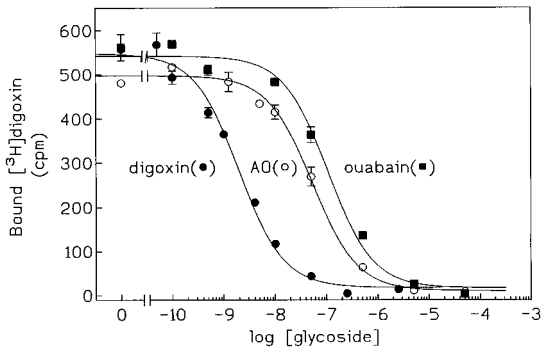

FIGURE 1: Determination of the affinities of the anti-digoxin mAb 26-10 for digoxin, ouabain, and AO using a competitive radioligand binding assay. The curves show the inhibition of [^{3}H]digoxin (5 nM) binding to mAb 26-10 (0.006 μg/0.5 mL) by increasing concentrations of digoxin (●), ouabain (■), and AO (○). The assays were performed in 0.5 mL of PBS (pH 7.4) with 0.05% BSA added as a carrier protein. The ordinate shows the [^{3}H]digoxin (counts per minute) bound to mAb in the absence and presence of varying concentrations of competing, unlabeled glycoside. Each data point shown is the mean of two determinations.

Table 1: K_i's of Digoxin, Ouabain, and AO for mAbs[a]

mAb	digoxin K_i (nM)	ouabain K_i (nM)	AO K_i (nM)
26-10	0.09 ± 0.05	3.26 ± 0.74	1.22 ± 0.19
45-20	0.02 ± 0.01	0.92 ± 0.18	0.19 ± 0.07
40-50	0.16 ± 0.13	2.22 ± 0.04	0.36 ± 0.3

[a] The values were determined using a competitive radioligand binding assay (see Materials and Methods).

of the digoxin binding sites of these mAbs. This was accomplished using a competitive radioligand ([^{3}H]digoxin) binding assay, with a double antibody precipitation of the anti-digoxin mAbs. Figure 1 shows [^{3}H]digoxin binding to mAb 26-10 as a function of increasing concentrations of the competing ligands digoxin, ouabain, and AO. The order of their binding affinities as based on the K_i values obtained was digoxin > AO > ouabain. The K_i values of these three ligands for mAbs 45-20 and 40-50 (see Table 1) were similarly obtained. All three mAbs were found to have a higher affinity for AO than for ouabain, and the order of the mAbs with respect to their affinities for AO was 45-20 > 40-50 > 26-10. These data showed that all three mAbs bind AO with high affinities, and the K_i values obtained for digoxin and ouabain compare well with those previously published by Schildbach et al. (*27*) and Jeffrey et al. (*29*). In contrast, the affinity of Na^+,K^+-ATPase for AO, which was determined to be 9 nM by Amler et al. (*33*; unpublished results) using spectroscopic methods, is lower than that of these mAbs.

Determination of Fluorescence Emission Spectra of Free and Protein-Bound AO. Free AO has a low fluorescence intensity in aqueous media with excitation and emission maxima of 364 and 485 nm, respectively. To determine the effects of protein binding upon AO fluorescence, AO (0.3 μM) was first titrated with increasing concentrations of Na^+,K^+-ATPase and mAbs 26-10, 45-20, and 40-50 until saturation of AO binding was achieved (data not shown). The binding of AO to excess Na^+,K^+-ATPase and mAb 26-10 resulted in a 3.0- and 3.5-fold increase, respectively, in its fluorescence intensity, accompanied by a blue shift in its emission maximum from 485 to 470 nm (see Figure 2). AO binding to mAb 45-20 resulted in a 1.9-fold increase in its

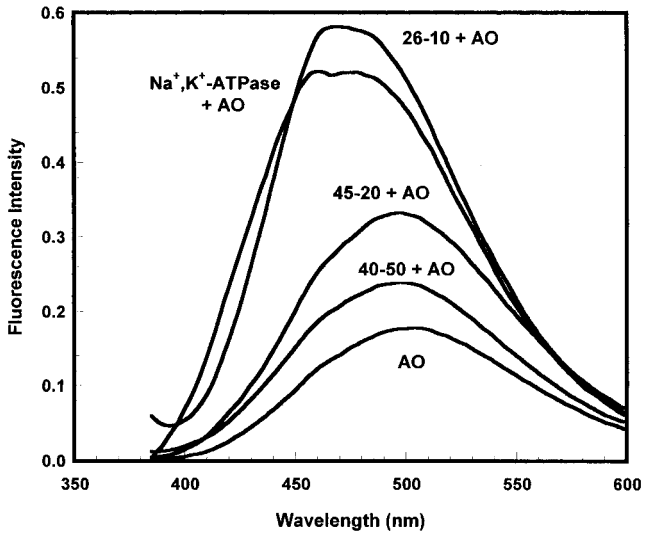

FIGURE 2: Emission spectra of free and protein-bound AO. The fluorescence emission spectra (λ_{ex} = 364 nm) of 0.3 μM AO in buffer and AO saturated with excess Na^+,K^+-ATPase (0.6 μM), mAb 26-10 (0.6 μM), mAb 45-20 (0.6 μM), and mAb 40-50 (2.0 μM) are as shown. The buffer was 50 mM Tris and 1 mM EGTA (pH 7.4) with 5 mM $MgCl_2$ and P_i added for AO binding to Na^+,K^+-ATPase.

fluorescence intensity without any significant shift in the emission maximum. However, despite the high affinity of AO for mAb 40-50 (see Table 1), only a small enhancement in AO fluorescence (F/F_0 = 1.1) was seen to occur upon its binding to mAb 40-50, thereby precluding further characterization of AO binding to this mAb. In all cases, excess, unlabeled ouabain (30−60 μM) blocked specific binding of AO (data not shown). As AO also binds nonspecifically to the lipids associated with Na^+,K^+-ATPase (*32*), the spectra of AO bound to Na^+,K^+-ATPase were obtained in the presence and absence of excess ouabain (60 μM) to correct for the contributions of nonspecific binding. These data provided the first indication that the AO binding environment in Na^+,K^+-ATPase is similar to that in mAb 26-10 but not in mAbs 45-20 and 40-50.

Determination of the Fluorescence Emission Decay Lifetimes of Free and Protein-Bound AO. To further characterize the effects of the local protein environments of mAbs 26-10 and 45-20 and Na^+,K^+-ATPase on bound AO fluorescence, the fluorescence decay lifetime(s) (τ) and fluorescence polarization (r) of the AO−protein complexes were measured. Frequency domain fluorometry revealed that the fluorescence of free AO decayed as a double exponential with an average lifetime (τ_{av}) of 0.6 ns (see Table 2). These results are consistent with the biexponential AO fluorescence decay reported previously by Amler et al. (*33*) showing that a complex lifetime decay is intrinsic to the free probe and not due to its binding to protein. Analyses of the phase and modulation data obtained for the AO−protein complexes (see Table 2) once again indicated a biexponential fluorescence decay as triexponential fits of the data did not significantly improve the χ^2 (goodness-of-fit parameter) values.

As shown in Table 2, the binding of AO to Na^+,K^+-ATPase and mAb 26-10 resulted in a 9.5- and 18.8-fold increase, respectively, in its average fluorescence lifetime. In both cases, these increases in τ_{av} are attributed to an increased τ_1 value and an increase in the extent (fractional

Table 2: Excited-State Lifetimes (τ) of AO Bound to Na^+,K^+-ATPase and mAbs[a]

sample	decay time τ (ns)	fractional intensity f	average lifetime τ_{av} (ns)	fold increase in τ_{av} $[\tau_{av}/\tau_{av(0)}]$
AO	$\tau_1 = 1.5$	$f_1 = 0.30$	0.6	–
	$\tau_2 = 0.2$	$f_2 = 0.70$		
AO and Na^+,K^+-ATPase	$\tau_1 = 6.6$	$f_1 = 0.85$	5.7	9.5
	$\tau_2 = 0.7$	$f_2 = 0.15$		
AO and mAb 26-10	$\tau_1 = 15.7$	$f_1 = 0.71$	11.3	18.8
	$\tau_2 = 0.6$	$f_2 = 0.29$		
AO and mAb 45-20	$\tau_1 = 2.2$	$f_1 = 0.59$	1.5	2.5
	$\tau_2 = 0.5$	$f_2 = 0.41$		

[a] To determine the rate(s) of AO fluorescence emission decay, the frequency response of the fluorescence of free AO (0.8 μM) and AO with excess protein (1.0−1.6 μM) was measured over a range of modulation frequencies (see Materials and Methods for details). τ_{av} represents the average fluorescence lifetime, and $\tau_{av(0)}$ represents the average lifetime of free AO. The buffer was 50 mM Tris and 1 mM EGTA (pH 7.4) with 5 mM $MgCl_2$ and P_i added for measurements with Na^+,K^+-ATPase.

Table 3: Effect of AO Binding to Na^+,K^+-ATPase and mAbs on Its Anisotropy (r)[a]

sample	anisotropy (r)
AO in buffer	0.078 ± 0.003
AO and Na^+,K^+-ATPase	0.158 ± 0.004
AO and mAb 26-10	0.173 ± 0.002
AO and mAb 45-20	0.193 ± 0.002

[a] The anisotropy (r) values of free AO (0.3 μM) and bound AO were determined at increasing protein concentrations using an ISS Greg K2 spectrofluorometer (see Materials and Methods). The r values reported are for AO saturated with protein (0.5 μM). Each r value is the mean of five measurements.

intensity, f_1) to which τ_1 contributes to the total emission. The increase in the τ_{av} value of AO to 5.7 ns upon binding to Na^+,K^+-ATPase is in agreement with the τ_{av} value of 5.8 ns reported previously by Amler et al. (*33*). However, the 9.5- and 18.8-fold increases in the average AO fluorescence lifetime are greater than the 3.0- and 3.5-fold increases in its steady-state fluorescence upon binding to Na^+,K^+-ATPase and mAb 26-10, respectively (see Figure 2). This suggests that some static quenching of AO may be occurring upon complexation, in addition to an increase in τ_{av}. In contrast to the large increase in τ_{av} seen upon AO binding to Na^+,K^+-ATPase and mAb 26-10, AO binding to mAb 45-20 resulted in a smaller, 2.5-fold increase in τ_{av} with less shift between the fractional intensities (see Table 2). Further, the increase in the average lifetime of AO was only marginally greater than the 1.9-fold enhancement of its fluorescence intensity upon binding to mAb 45-20 (see Figure 2). These results are consistent with the idea that the environments of AO in Na^+,K^+-ATPase and mAb 26-10 are similar but differ from that of AO in mAb 45-20.

Determination of the Fluorescence Anisotropies of Free and Protein-Bound AO. The anisotropy (r), or rotational freedom of a fluorophore, is dependent on the rigidity of the probe within its binding environment. The extent of polarization of bound AO fluorescence was, therefore, determined to further distinguish between these proteins. The increase in the r value of free AO from 0.078 to 0.158 or greater (see Table 3) observed upon titration of the probe with mAbs 26-10 and 45-20 and Na^+,K^+-ATPase is consistent with a decreased rotational mobility of the probe arising as a result of its binding to protein. However, while it was not possible to make specific distinctions between the mAbs on the basis of the r values, both Na^+,K^+-ATPase and mAb 26-10 placed less rotational restrictions on bound AO than mAb 45-20. For perspective, the r values obtained for these noncovalent AO−protein binding interactions are similar to the r values of 0.17 and 0.176 obtained for 5′-iodoacetamidofluorescein (5′-IAF) (*41*) and Lucifer Yellow (*33*) covalently bound to the Na^+,K^+-ATPase α subunit Cys-457 and β carbohydrates, respectively, but significantly lower than the r value of 0.36 reported by Abbott et al. (*42*) for fluorescein 5′-isothiocyanate (FITC) covalently linked to the Na^+,K^+-ATPase α subunit Lys-501 (ATP binding domain). Therefore, the r values reported here are consistent with a decrease in the degree of rotational freedom of the anthroyl moiety arising from the location of AO in a binding cleft or pocket which is close to the surface of the proteins. Indeed, the X-ray crystal structures of structures of digoxin bound to Fab 26-10 (*28*) and ouabain bound to Fab 40-50 (*29*) show the lactone and steroid rings and a portion of the sugar moiety of these cardiac glycosides located in a superficial, water-free binding domain.

Measurement of Förster Resonance Energy Transfer (FRET) from Protein to AO. In addition to the spectral data obtained by the direct excitation of AO fluorescence, the fact that the emission spectrum of tryptophan (Trp) (λ_{em} = 340 nm) overlaps well with the absorption spectrum of AO (λ_{ex} = 364 nm) allows determination of long-range intermolecular, nonradiative Förster resonance energy transfer (FRET) between this donor (Trp) and acceptor (AO) pair (for review, see refs *38* and *39*). FRET determinations have been shown to be extremely useful in determining donor−acceptor distances as the rate and efficiency of energy transfer are inversely proportional to the sixth power of the distance between the donor and acceptor. The Förster critical distance (R_0), i.e., the donor−acceptor separation distance at which 50% of the excitation energy of the donor is transferred to the acceptor, was estimated to be 21 Å for the Trp−AO donor−acceptor pair, assuming relatively free rotation of both donor and acceptor (see Materials and Methods).

To further compare the binding sites of AO in the mAbs with the binding site in Na^+,K^+-ATPase, we determined if there was any FRET occurring from mAb Trp(s) to AO, in a manner analogous to that seen with the enzyme (*32*). Protein Trp fluorescence was selectively excited at 295 nm in the presence and absence of AO. The Trp fluorescence intensity of Na^+,K^+-ATPase (a total of 16 Trp residues with the α and β subunits combined) was observed to be ∼4-fold greater than that of an equimolar concentration of mAb 26-10 (24 Trp residues), suggesting that the Trp residues in mAb 26-10 were more quenched than those in the enzyme. Similarly, the Trp fluorescence intensities of mAbs 40-50 and 45-20 were ∼4- and 8-fold lower, respectively, than that of an equimolar concentration of Na^+,K^+-ATPase. Figure 3a shows the decrease in Na^+,K^+-ATPase donor (Trp) fluorescence emission (10.2%) at 340 nm as well as a distinct increase in acceptor (AO) fluorescence (observed at λs above 400 nm) resulting from the transfer of energy from excited Trp(s) of Na^+,K^+-ATPase to added AO. Excitation of intrinsic mAb 26-10 Trp fluorescence at 295 nm also resulted in a pronounced transfer of energy from excited mAb Trp(s) to AO, accompanied by a small decrease (3.4%) in Trp

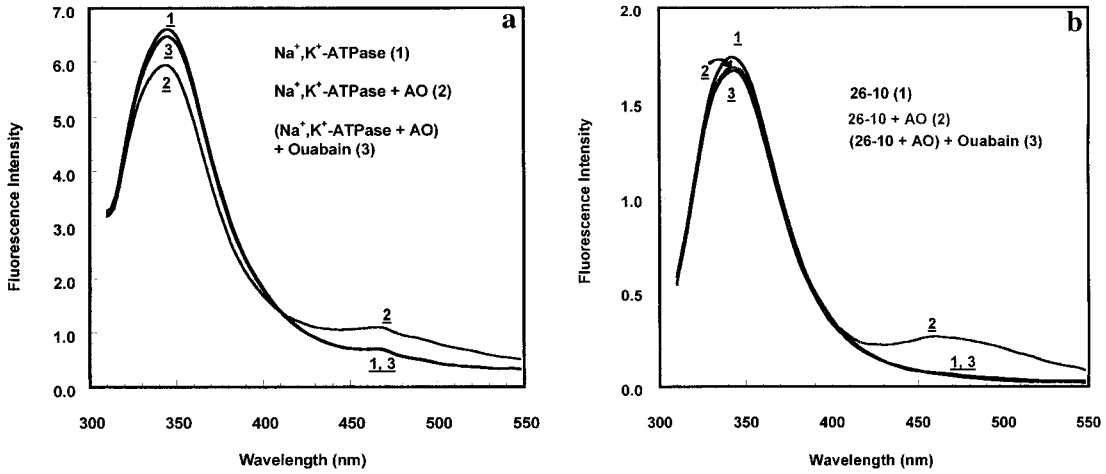

FIGURE 3: Förster resonance energy transfer from (a) Trp(s) in Na^+,K^+-ATPase to AO and (b) Trp(s) in mAb 26-10 to AO. The Trp fluorescence of Na^+,K^+-ATPase (0.6 μM) and mAb 26-10 (0.6 μM) was selectively excited at 295 nm in the absence (1) and presence (2) of 0.3 μM AO, and the resultant fluorescence emission was monitored between 310 and 550 nm as shown. Excess ouabain (60 μM) was added to reverse (3) the quenching of donor (Trp) fluorescence by the acceptor (AO). The buffer was 50 mM Tris-HCl (pH 7.4) and 1 mM EGTA with 5 mM $MgCl_2$ and P_i added for measurements with Na^+,K^+-ATPase.

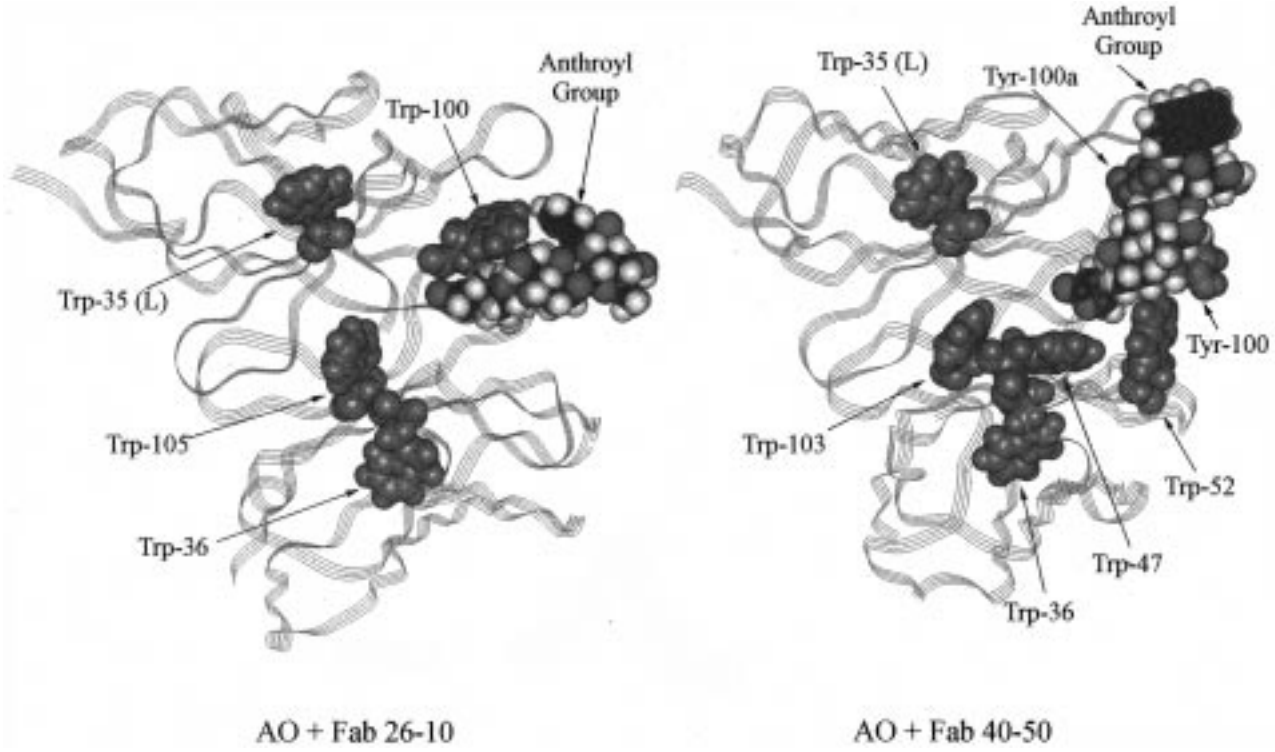

FIGURE 4: Models of AO binding to antigen-binding fragments (Fabs) of (a, left) mAb 26-10 and (b, right) mAb 40-50. Models were generated as previously described (see Materials and Methods). Heavy (H) and light chain (L) Trp residues are shown in orange, and Tyr residues H100*a* and H100 in Fab 40-50 are shown in pink. The lactone and steroid rings are buried in the mAb binding sites with the sugar (rhamnose) partially exposed to the solvent. The anthroyl group at position C-3 of the rhamnose is (a) ~3 Å from Trp-H100 in Fab 26-10 and (b) ~6 and 10 Å, respectively, from Tyr-H100*a* and Tyr-H100 and ~17 Å from Trp-H52 and Trp-L35 in Fab 40-50.

fluorescence emission (see Figure 3b). Similar FRET studies with mAbs 45-20 and 40-50 were quite distinct in that they showed that no transfer of energy from their Trp residue(s) to AO (data not shown) despite the presence of similar numbers of Trp residues. In control experiments, quenching of donor (Trp) fluorescence by the acceptor (AO) was prevented by prior addition of excess ouabain (60 μM) to both Na^+,K^+-ATPase and mAb 26-10 (see Figure 3a,b). However, unlike the case with the enzyme, the decrease in mAb 26-10 Trp fluorescence due to FRET was not fully reversed upon the addition of excess ouabain (see Figure 3b), as ouabain alone quenches ~2.5% of the mAb Trp fluorescence at these concentrations (data not shown).

Modeling of AO Binding to Antigen-Binding Fragments (Fabs) of Antibodies 26-10 and 40-50. To visualize the possible interaction(s) between the anthroyl moiety of AO and the mAb amino acid residues contributing to the AO fluorescence parameters measured above, we simulated AO binding to Fabs of antibodies 26-10 and 40-50. Models of the AO−mAb complexes were generated (see Figure 4a,b) as described (see Materials andMethods) using the known crystal structures of the digoxin−Fab 26-10 (*28*) and

ouabain−Fab 40-50 complexes (*29*). The AO−Fab complexes were first solvated and then refined by energy minimization calculations and dynamics simulations, followed by a second round of energy minimization calculations, to attain models of the most probable AO conformation in these complexes. The anthroyl moiety did not move from its initial position close to the edge of the 26-10 Fab antigen-binding pocket at the start of the dynamics simulations and continued to stay within ~3 Å of the heavy chain aromatic residue Trp-H100 for the duration of these simulations (see Figure 4a). Further, there was no apparent change with respect to the orientation of ouabain in the Fab relative to that of bound digoxin. Similar energy minimization and dynamics runs were also used to refine the model of AO binding to Fab 40-50. The model (see Figure 4b) revealed the absence of a Trp residue in the corresponding region of the mAb heavy chain and the presence of two Tyr residues, Tyr-H100*a* and Tyr-H100, at distances of ~6 and 10 Å, respectively, from the anthroyl moiety. The closest Trp residues, Trp-H52 and Trp-L35, are located ~17 Å from the anthroyl moiety. This distance gives a calculated efficiency of energy transfer (E) to AO of 84% and a 7% quenching of mAb 40-50 Trp fluorescence. However, the fact that no transfer of energy was seen upon excitation of mAb 40-50's Trp fluorescence suggests that these residues, together with the Trp residues (Trp-36, Trp-47, and Trp-103) located near the glycoside lactone moiety, may already be highly quenched.

DISCUSSION

The objective of this study was to determine whether the digoxin binding sites of mAbs are capable of mimicking that of the physiological receptor for cardiac glycosides, i.e., Na^+,K^+-ATPase. If this is the case, it may be possible to use this novel model receptor(s) system to determine the relationship between protein structure and high-affinity cardiac glycoside binding. The lack of a crystal structure for Na^+,K^+-ATPase coupled with the inability of photoaffinity labeling (*10*, *11*) site-directed mutagenesis studies of the ouabain-sensitive Na^+,K^+-ATPase α subunit (*13*−*22*), and studies using chimeric constructs of Na^+,K^+-ATPase (*23*, *24*) to identify the Na^+,K^+-ATPase cardiac glycoside binding site, underscores the need for alternative experimental approaches. Consequently, high-affinity anti-digoxin antibodies whose crystal structures are known are good candidates for study as potential models of the cardiac glycoside receptor.

Fortes (*32*) and Amler et al. (*33*; unpublished results) have shown that AO binds Na^+,K^+-ATPase in the presence of Mg^{2+} and P_i with a nanomolar affinity essentially identical to that of ouabain. Our radioligand binding data indicate that the presence of the fluorescent anthroyl moiety at C-3 of the sugar (rhamnose) of ouabain, likewise, does not hinder its binding to the three mAbs studied, and in fact, AO binds to these mAbs with affinities higher than that of ouabain. However, these antibodies are different from Na^+,K^+-ATPase in that they show a pronounced preference for digoxin over other cardiac glycosides (*26*). Our results indicate that the affinities of mAbs 45-20, 40-50, and 26-10 for digoxin (their original antigen) are 14-, 46-, and 36-fold greater, respectively, than their affinities for ouabain. The enzyme, despite species variations, rarely shows a more than 2-fold difference (*43*, *44*) in its affinity for digoxin and ouabain. In addition, unlike Na^+,K^+-ATPase, these mAbs do not undergo ligand-dependent conformational changes that alter their glycoside binding affinities (*28*, *29*).

Although mAb 26-10 has the lowest affinity (K_i) for AO of the three mAbs studied, our spectroscopic data show that only it, like Na^+, K^+-ATPase, binds AO, producing a large increase in its fluorescence intensity ($F/F_0 = 3.5$) and a blue shift in its emission maximum. This indicates that in both proteins the binding of AO places the anthroyl moiety in a less solvent-exposed and more hydrophobic environment. This is also consistent with the idea that binding of cardiac glycoside to the physiological receptor, i.e., Na^+,K^+-ATPase, occurs in a hydrophobic cleft (*7*). The enhancements in AO fluorescence seen upon AO binding to Na^+,K^+-ATPase and mAb 26-10 are also reflected in the dramatic increases in the average AO fluorescence decay lifetime from 0.6 ns to 5.7 and 11.3 ns, respectively. These 9.5- and 18.8-fold increases in average AO fluorescence lifetimes upon binding Na^+,K^+-ATPase and mAb 26-10 can be, similarly, attributed to the existence of a hydrophobic environment in the vicinity of the anthroyl group. Interestingly, the high-affinity binding of AO to mAbs 45-20 and 40-50 produces much smaller increases in its fluorescence intensity without any blue shift in its emission maximum, suggesting that the immediate environment of the bound probe in these antibodies is less hydrophobic. The considerably smaller, i.e., 2.5-fold increase in the average fluorescence lifetime of AO complexed to mAb 45-20, is consistent with this idea.

Fluorescence anisotropy measurements show that mAbs 26-10 and 45-20 and Na^+,K^+-ATPase bind AO with similar increases in AO rigidity, suggesting that the differences in AO fluorescence enhancement seen with mAbs 26-10 and 45-20 can be primarily attributed to differences in the polarity of the environment of the anthroyl moiety in these mAbs and not to differences in their AO-binding affinities which are 1.22 (mAb 26-10) and 0.19 nM (mAb 45-20), respectively. As discussed earlier, the magnitude of the difference in the extent of polarization of the probe upon binding to either mAb 26-10 or 45-20 ($r = 0.17$ or 0.19, respectively) is not sufficient to distinguish between them with respect to their binding of AO. However, the slightly higher r value for AO bound to mAb 45-20 suggests a more restrictive binding interaction.

Förster resonance energy transfer (protein Trp to AO) studies by Fortes (*32*) and Trp-dependent photoaffinity labeling studies of Na^+,K^+-ATPase with *p*-aminobenzenediazonium (ABD)−ouabain by Goeldner et al. (*45*) have implied that one or more Trp residues are located at or near the cardiac glycoside binding site. More recently, however, mutation of the conserved Trp-310 which is in the second extracellular loop of the sheep α1 subunit of Na^+,K^+-ATPase and is a likely candidate for interacting with the glycosides was shown to have no effect on the ouabain binding affinity (*46*). Our data showing significant Förster energy transfer from Trp residue(s) of lamb kidney Na^+,K^+-ATPase to AO are consistent with at least one Trp residue being close to the AO-binding site in Na^+,K^+-ATPase, but it does not provide any information on its involvement in the binding interaction. The fact that there are a total of 12 Trp residues in the α subunit and 4 in the β subunit of the Na^+,K^+-ATPase and that their relative contributions to the energy transfer process are not known makes the calculation of a definite

distance between one or more contributing Trp residue(s) and AO difficult. However, estimates of the approximate numbers of Trp residues involved can be made on the basis of the efficiencies of the observed energy transfer, assuming that all the Trp residues in Na^+,K^+-ATPase are contributing equally to the fluorescence signal. The observed energy transfer from Trp residues in Na^+,K^+-ATPase to bound AO is 10.2%, which is more than sufficient to completely quench the fluorescence of at least one Trp residue, placing it a distance of ~10 Å or less from the anthroyl moiety. If only 2 out of the 16 Na^+,K^+-ATPase Trp residues are involved in the energy transfer process, this would result in a transfer efficiency of about 82% for each Trp and place them at an average distance (R_{av}) of ~17 Å from the anthroyl moiety.

The appearance of AO fluorescence emission upon excitation of the intrinsic fluorescence of mAb 26-10 and not mAbs 45-20 and 40-50 suggests that one or more Trp residues is uniquely located in the vicinity of the AO-binding site in mAb 26-10 with relative orientations of AO and Trp residue(s) similar to those in Na^+,K^+-ATPase. Consistent with this, the crystal structure of digoxin bound to Fab 26-10 shows a Trp residue (Trp-H100) on the edge of the binding site making contact with the lactone and steroid backbone of digoxin (*28*). In contrast, the crystal structure of ouabain bound to Fab 40-50 shows two Tyr residues (Tyr-H100 and Tyr-H100*a*) located in the mAb binding site, making contacts with either the sugar moiety and steroid backbone of digoxin or the sugar moiety alone (*29*). It is likely, therefore, that the absence of a Trp residue in this region of mAb 40-50 is responsible for the differences in the fluorescence properties of AO bound to mAbs 26-10 and 40-50. Although the complete amino acid sequence and X-ray crystal structure of mAb 45-20 is not available at this time, we hypothesize that its heavy chain, likewise, does not contain a Trp residue at position H100.

We have generated models of AO in Fabs 26-10 and 40-50 using the published crystal structures of digoxin bound to Fab 26-10 (*28*) and ouabain bound to Fab 40-50 (*29*) to investigate the contributions of mAb structure to the observed changes in AO fluorescence upon binding. Our model of AO bound to Fab 26-10 suggests that Trp-H100, which is located on the surface of the mAb, is a distance of ~3 Å from the anthroyl moiety with its short axis perpendicular to it. The Förster critical distance, i.e., the Trp−AO donor−acceptor separation distance at which 50% of the excitation energy of the donor is transferred to the acceptor, was estimated to be 21 Å. This suggests that Trp-H100 should very easily meet both distance and donor−acceptor orientation (parallel or perpendicular to each other) criteria necessary for significant energy transfer to occur (for review, see refs *38* and *39*). In fact, the calculated efficiency (E) of energy transfer based on an R value of 3 Å is 99.9%. Assuming that all of the 24 Trp residues in mAb 26-10 contribute equally to the Trp fluorescence signal, complete transfer by one Trp residue would cause a 4.2% fluorescence decrease in the observed signal. This is consistent with the observed 3.4% quenching of mAb Trp fluorescence which gives an E value of 81% and is in agreement with our modeling studies. In contrast, an average Trp−AO distance (R_{av}) of ~38 Å is obtained if the FRET is simply averaged over all Trp residues in mAb 26-10. Our model also suggests that the interaction of the hydrophobic anthroyl moiety of AO with the aromatic Trp-H100 residue prolongs the lifetime of the excited state of AO, resulting in an increase in its fluorescence intensity and a blue-shifted emission maximum. The absence of Förster energy transfer between mAb 40-50 and AO is consistent with the absence of a Trp residue in the corresponding region of the mAb heavy chain. In addition, it suggests either that the 5 Trp residues which are located close enough (17−20 Å) to the anthroyl moiety for efficient energy transfer to occur are not in the appropriate orientation for transfer to occur or that their fluorescence is already quenched. It appears, therefore, that the location of a Trp residue at position 100 in the mAb 26-10 heavy chain is crucial for energy transfer and suggests that mAb Trp residue(s) must be located a distance of less than 17 Å from the anthroyl moiety for FRET to occur.

Anti-digoxin mAbs bind glycosides by burying the hydrophobic lactone and steroid rings in the antibody-combining site while leaving the hydrophilic sugar moiety largely exposed to solvent (*28*, *29*). It is believed that cardiac glycosides bind Na^+,K^+-ATPase either at a hydrophobic cleft in the protein surface or by partially inserting their hydrophobic surfaces into the lipid bilayer between transmembrane segments with the hydrophilic sugar moiety(s) partly exposed to solvent (*7*). It has also been proposed that high-affinity binding of the cardiac glycosides to Na^+,K^+-ATPase requires the presence of a lipid barrier over the binding site (*47*). The AO−mAb 26-10 binding data suggest that the presence of lipids in the immediate vicinity of the cardiac glycoside sugar moiety(s) may not be essential for duplication of the physical environment surrounding the glycoside sugar(s) in the enzyme. Furthermore, the data also indicate that for efficient energy transfer to occur between Trp residue(s) in Na^+,K^+-ATPase and AO, one or more Trp residues must be situated less than 17 Å from the anthroyl moiety of ouabain. Although it is not clear at the present time whether any of the contributing Trp residues in Na^+,K^+-ATPase are a determinant of oubain sensitivity, our model shows that Trp-H100 in mAb 26-10 interacts with the anthroyl group of ouabain. Trp-H100 has also been shown to be located in the mAb cardiac glycoside binding pocket, making contact with the lactone and steroid backbone of digoxin (*28*). Studies are underway, using site-directed mutagenesis, to determine whether Trp-H100 in mAb 26-10 is responsible for the observed changes in AO fluorescence and is a determinant of AO binding affinity. It will be interesting to determine whether replacement of Tyr-H100 and/or Tyr-H100*a* in the heavy chain of mAb 40-50 with Trp will produce changes in AO fluorescence similar to those seen with AO binding to mAb 26-10.

In conclusion, the similarities in the fluorescence properties of AO bound to either mAb 26-10 or Na^+,K^+-ATPase indicate that an anti-digoxin antibody can duplicate many of the properties of the physiological receptor. This anti-digoxin antibody could, therefore, serve as a model receptor for the study of cardiac glycoside binding to Na^+,K^+-ATPase.

ACKNOWLEDGMENT

We thank Dr. Alan Abbott for helpful suggestions and calculation of the Trp−AO Förster critical distance (R_0). A portion of this paper was presented at the VIIIth International

Conference on the Na^+/K^+-ATPase, Mar del Plata, Argentina, 1996.

REFERENCES

1. Pedersen, P. L., and Carafoli, E. (1987) *Trends Biochem. Sci. 12*, 146−150.
2. Green, N. M. (1992) in *Ion-Motive ATPases: Structure, Function and Regulation* (Scarpa, A., Carafoli, E., and Papa, S., Eds.) p 104, New York Academy of Sciences, New York.
3. Lingrel, J. B., and Kuntzweiler, T. (1994) *J. Biol. Chem. 269*, 19659−19662.
4. Sweadner, K. J. (1989) *Biochim. Biophys. Acta 988*, 185−220.
5. McDonough, A. A., Geering, K., and Farley, R. A. (1990) *FASEB J. 4*, 1598−1605.
6. Lingrel, J. B., Orlowski, J., Shull, M. M., and Price, E. M. (1990) *Prog. Nucleic Acid Res. Mol. Biol. 38*, 37−89.
7. Thomas, R., Gray, P., and Andrews, J. (1989) *Adv. Drug Res. 19*, 311−562.
8. Hoffman, J. F. (1966) *Am. J. Med. 41*, 666−680.
9. Wallick, E. T., Pitts, B. J. R., Lane, L. K., and Schwartz, A. (1980) *Arch. Biochem. Biophys. 202*, 442−449.
10. Forbush, B., III (1983) in *Current Topics in Membranes and Transport* (Hoffman, J. F., and Forbush, B., III, Eds.) Vol. 19, pp 167−201, Academic Press, New York.
11. Hansen, O. (1984) *Pharmacol. Rev. 36*, 143−163.
12. Antolovic, R., Linder, D., Hahnen, J., and Schoner, W. (1995) *Eur. J. Biochem. 227*, 61−70.
13. Price, E. M., and Lingrel, J. B. (1988) *Biochemistry 27*, 8400−8408.
14. Price, E. M., Rice, D. A., and Lingrel, J. B. (1989) *J. Biol. Chem. 264*, 21902−21906.
15. Price, E. M., Rice, D. A., and Lingrel, J. B. (1990) *J. Biol. Chem. 265*, 6638−6641.
16. Canessa, C. M., Horisberger, J. D., Louvard, D., and Rossier, B. C. (1992) *EMBO J. 11*, 1681−1687.
17. Schultheis, P. J., and Lingrel, J. B. (1993) *Biochemistry 32*, 544−550.
18. Schultheis, P. J., Wallick, E. T., and Lingrel, J. B. (1993) *J. Biol. Chem. 268*, 22686−22694.
19. Burns, E. L., and Price, E. M. (1993) *J. Biol. Chem. 268*, 25632−25635.
20. Feng, J., and Lingrel, J. B. (1994) *Biochemistry 33*, 4218−4224.
21. Askew, G. R., and Lingrel, J. B. (1994) *J. Biol. Chem. 269*, 24120−24126.
22. Canessa, C. M., Horisberger, J. D., and Rossier, B. C. (1993) *J. Biol. Chem. 268*, 17722−17726.
23. Blostein, R., Zhang, R., Gottardi, C. J., and Caplan, M. J. (1993) *J. Biol. Chem. 268*, 10654−10658.
24. Ishii, T., and Takeyasu, K. (1993) *Proc. Natl. Acad. Sci. U.S.A. 90*, 8881−8885.
25. Smith, T. W., Haber, E., Yeatman, L., and Butler, V. P., Jr. (1976) *N. Engl. J. Med. 294*, 797−800.
26. Mudgett-Hunter, M., Anderson, W., Haber, E., and Margolies, M. N. (1985) *Mol. Immunol. 22*, 477−488.
27. Schildbach, J. F., Panka, D. J., Parks, D. R., Jager, G. C., Novotny, J., Herzenberg, L. A., Mudgett-Hunter, M., Bruccoleri, R. E., Haber, E., and Margolies, M. N. (1991) *J. Biol. Chem. 266*, 4640−4647.
28. Jeffrey, P. D., Strong, R. K., Sieker, L. C., Chang, C. Y. Y., Campbell, R. L., Petsko, G. A., Haber, E., Margolies, M. N., and Sheriff, S. (1993) *Proc. Natl. Acad. Sci. U.S.A. 90*, 10310−10314.
29. Jeffrey, P. D., Schildbach, J. F., Chang, C. Y. Y., Kussie, P. H., Margolies, M. N., and Sheriff, S. (1995) *J. Mol. Biol. 248*, 344−360.
30. Short, M. K., Jeffrey, P. D., Kwong, R. F., and Margolies, M. W. (1995) *J. Biol. Chem. 270*, 28541−28550.
31. Jerne, N. K. (1974) *Ann. Immunol. (Paris) 125C*, 373−389.
32. Fortes, P. A. G. (1977) *Biochemistry 16*, 531−540.
33. Amler, E., Abbott, A., Malak, H., Lackowicz, J., and Ball, W. J., Jr. (1996) *Biophys. J. 70*, 182−193.
34. Lane, L. K., Potter, J. D., and Collins, J. H. (1979) *Prep. Biochem. 9*, 157−190.
35. Lowry, O. H., Rosebrough, N. J., Farr, A. L., and Randall, R. J. (1951) *J. Biol. Chem. 193*, 265−275.
36. Abbott, A., and Ball, W. J., Jr. (1993) *Biochemistry 32*, 3511−3518.
37. Cheng, Y.-C., and Prusoff, W. H. (1973) *Biochem. Pharmacol. 22*, 3099−3108.
38. Lackowicz, J. R. (1983) in *Principles of Fluorescence Spectroscopy*, Plenum Press, New York.
39. Stryer, L. (1968) *Science 162*, 526−533.
40. Lackowicz, J. R., Gratton, E., Lackzo, G., Cherek, H., and Limkemann, M. (1984) *Biophys. J. 46*, 463−477.
41. Amler, E., Abbott, A., and Ball, W. J., Jr. (1992) *Biophys. J. 61*, 553−568.
42. Abbott, A., Amler, E., and Ball, W. J., Jr. (1992) *Biochemistry 31*, 11236−11243.
43. Brown, L., Erdman, E., and Thomas, R. (1983) *Biochem. Pharmacol. 32*, 2767−2774.
44. Palasis, M., Kuntzweiler, T. A., Argüello, J. M., and Lingrel, J. (1996) *J. Biol. Chem. 271*, 14176−14182.
45. Goeldner, M. P., Hirth, C. G., Rossi, B., Ponzio, G., and Lazdunski, M. (1983) *Biochemistry 22*, 4685−4690.
46. Lingrel, J. B., Orlowski, J., Price, E. M., and Pathak, B. G. (1990) in *The Sodium Pump: Structure, Mechanism and Regulation* (Kaplan, J. H., and De Weer, P., Eds.) Vol. 46, Part 1, pp 1−16, The Rockefeller University Press, New York.
47. Akera, T., Tobin, T., Gatti, A., Shieh, I. S., and Brody, T. M. (1974) *Mol. Pharmacol. 10*, 509−518.

BI973037D